ISSN 1063-7834, Physics of the Solid State, 2013, Vol. 55, No. 8, pp. 1747–1753. © Pleiades Publishing, Ltd., 2013.
Original Russian Text © M.V. Baidakova, Yu.A. Kukushkina, A.A. Sitnikova, M.A. Yagovkina, D.A. Kirilenko, V.V. Sokolov, M.S. Shestakov, A.Ya. Vul', B. Zousman, O. Levinson, 2013, published in Fizika Tverdogo Tela, 2013, Vol. 55, No. 8, pp. 1633–1639.

ATOMIC CLUSTERS

Structure of Nanodiamonds Prepared by Laser Synthesis

M. V. Baidakova[a], Yu. A. Kukushkina[a], A. A. Sitnikova[a], M. A. Yagovkina[a], D. A. Kirilenko[a], V. V. Sokolov[a], M. S. Shestakov[a], A. Ya. Vul'[a, *], B. Zousman[b], and O. Levinson[b]

[a] *Ioffe Physical-Technical Institute, Russian Academy of Sciences, Politekhnicheskaya ul. 26, St. Petersburg, 194021 Russia*

* *e-mail: alexandervul@mail.ioffe.ru*

[b] *Ray Techniques Ltd, Building 4–2, High Tech Village, The Hebrew University of Jerusalem, P.O.B. 39162, Jerusalem, 91391 Israel*

Received February 25, 2013

Abstract—A study is reported of nanodiamonds obtained by a new method—pulsed laser ablation of a specially prepared carbon target. In the mechanism employed to produce a diamond phase, this method is similar to that of detonation synthesis of nanodiamonds. The main structural characteristics of the material have been determined and compared with the corresponding characteristics of detonation nanodiamonds.

DOI: 10.1134/S1063783413080027

1. INTRODUCTION

The recent decade has revealed a stable interest in investigation of the structure of diamond powders and suspensions with a characteristic size of crystal grains less than 100 nm, the so-called nanodiamonds (NDs) [1].

This interest is stimulated primarily by the continuously growing list of possible nanodiamond applications. Besides the fairly obvious use of nanodiamonds for mirror polishing, as a component of antifriction liquids and precursors employed in growing diamond films by chemical vapor deposition (CVD), we are witnessing an ever growing attention to bio-medical ND applications as biomarkers and drug delivery vehicles [2].

Until quite recently the most extensively employed industrial method of NDs production was the detonation method, in which the ND are synthesized in detonation of strong explosives in a closed volume at a negative oxygen balance [3]. The average size of crystallites of detonation nanodiamond (DND) is 3–5 nm, but the suspensions prepared from industrial DND powders contain substantially larger agglomerates ranging to more than 100 nm in size. The difficulty plaguing DND deaggregation in solvents represents the principal obstacle on the way to substantial broadening of their already wide application in various areas. For instance, it is only in the recent years that one has succeeded in preparing stable water suspensions with particles less than 10 nm in size [4–6]. Moreover, it is progress reached in DND deaggregation that gives promise to a successful solution of the problem of removing metal impurities from DND. It is pointed out [7] that removal of metal impurities is one of the most arduous and technically demanding stages in DND production.

A comparatively recent achievement was the solution, at any rate, in laboratory conditions, to the problem of obtaining NDs by crushing and fractionation of microcrystalline diamond powders produced by a method enjoying wide application in engineering practice and based on high-pressure and temperature synthesis from graphite [8].

The present paper puts forth the results of investigation of diamond nanopowders prepared by pulsed laser ablation of a solid target, which we are going to call in what follows laser nanodiamonds (LND). We will also compare the structures of the DND and LND. This comparison appears to be justified not only by the nanometer-scale dimensions of diamond crystallites but also, considered from a physical viewpoint, by the method involving pulsed laser ablation (PLA) of a solid target being similar to that of detonation synthesis; indeed, formation of a crystallite of crystal atoms takes place at a high pressure building up in a shock wave [9].

The appearance of the PLA method is directly related to development of high-power rubidium lasers in the early 1960s. The interest to this technological method has recently grown because the PLA permits one, in principle, to vary easily the parameters of synthesis and produce nanodiamonds free of metal impurities. Until quite recently, however, application of the PLA to engineering-scale ND production was believed economically unreasonable.

We are reporting here on a study of LND obtained by the new method involving laser ablation of a specially prepared target rather than of graphite [10]. Here, the laser beam is focused in the layer of an optically transparent liquid at a fixed distance from the target surface. Thus, the target is treated not by the

plasma but rather by a high-power hydroshock produced by the laser light pulse (the light-hydraulic effect [11]). Application of the light-hydraulic effect with a specially treated target to ND production by the PLA method has brought about a substantial increase of ND output, thus opening promise to industrial application of PLA.

2. TECHNIQUE OF SAMPLE PREPARATION

The LND samples to be studied were prepared by the method similar to the one described in [12], i.e., by laser ablation of a specially prepared target containing diamond-free carbon soot and a hydrocarbon binder under a layer of an optically transparent liquid.

A pulsed solid-state YAG laser operating at 1064 nm was employed in the synthesis, with the stage with the target fixed to it moving automatically in such a way that the laser spot scanned the liquid above its surface.

The synthesized LND particles were separated by flotation in deionized water, rinsed and dried.

Three LND samples were studied. LND samples 1 and 2 differed in target composition. Sample 2 was obtained by treating of the target containing the hydrocarbon binder with an addition of stearine acid. One could expect in this case a variation of chemical groups on the surface of LND particles. We note immediately that adding an insignificant amount of stearine acid in the course of target preparation brought about an increase of nanodiamond yield by almost 50%.

The target for sample 3 was prepared by the technique used with sample 1, but without the stearine acid. In contrast to sample 1, the scanning step, i.e. the distance between hydroshocks, was reduced by one half, which resulted in a decrease of the synthesis efficiency. The step with samples 1 and 2 was 30 μm, and that with sample 3 was 15 μm.

To compare the relevant structural characteristics, the paper presents data obtained in studies of commercial DND samples produced by FGUP SKTB "Tekhnolog," St. Petersburg The DND samples were prepared by the standard technique involving detonation of a mixture of trinitrotoluene with hexogen (50/50 ratio), and nanodiamonds were isolated from detonation carbon (DC) with CrO_3 solution in sulfuric acid.

3. EXPERIMENTAL TECHNIQUE

The X-ray diffraction was studied with a Geigrflex D/max-RC diffractometer Rigaku Co (Japan) with the following instrument settings: monochromatized CuK_α radiation (λ = 1.541 mÅ); stepped scanning, time of signal accumulation at one point 2 s, recording step 0.02°, current and accelerating voltage at the X-ray tube—70 mA and 40 kV; scanning interval 3°–120° in 2θ; divergence slit (DS) = 1°; Soller slit (SS) = 0.15°; receiving slit (RS) = 1°. The unit cell parameters were determined by the internal standard method, with 99.95%-pure silicon powder used as the standard.

Microphotographs of the samples were obtained with Philips EM-400 (accelerating voltage 100 kV) and Jeol JEM-2100F (accelerating voltage 200 kV, spatial resolution 1.2 Å) transmission electron microscopes. The samples in the form of suspension in a water solution were deposited onto a supporting carbon film prepared from graphite oxide directly on special copper grids used in electron microscopy. The coating thus formed is stable under electron beam irradiation and reveals a high transparency for electrons [13]. The samples intended for measurement of IR transmission spectra were pellets (13 mm in diameter) prepared by conventional pressing of nanodiamond and KBr (Uvasol®, Merck) powders in vacuum.

The distribution of nanodiamond particles by dynamic light scattering (DLS) was measured with a Malvern Zetasizer ZS 3600 instrument. The instrument was calibrated against standard samples US NIST 60 nm and 200 nm, as well as against polysaccharide and polymer (polyvinylpyrrolidone) molecules with known characteristics. Water suspensions of LND were obtained by ultrasonic dispersion of LND powder in deionized water. The fraction of LND in the samples was about 0.03% of the mass of their water suspensions.

The pycnometric density d_p was determined by gas (helium) pycnometry with the AccuPyc 1330 instrument. The samples were preliminarily dried to a constant mass at 105°C.

The elemental composition of the samples was derived from REM (REM FEI QANTA 200 equipped with an EDAX analyzer). The instrument permits identification of elements starting with boron. The sensitivity of determination is 0.02 wt %.

The specific surface S_s was extracted from data obtained in measurements of low-temperature adsorption of nitrogen (at 77 K) and argon (at 87 K) with an ASAP 2020 analyzer. The samples under study were first subjected to degassing in vacuum at 300°C for 24 h. The specific surface was calculated by the Brunauer–Emmett–Teller (BET) method [14] within the range of relative pressures of nitrogen or argon of 0.05–0.30.

4. RESULTS AND DISCUSSION

All the samples, both obtained by PLA and by the detonation method, were grey powders. The samples did not differ from one another either in color or in particle size, which permitted application of the same sample preparation methods.

As follows from the elemental composition of the LND and DND samples, all the samples are actually

carbon material (carbon content above 95%) and contain a significant amount of oxygen (2–4%).

Note that LND samples are practically free of impurities, whereas the presence of impurities in the DND sample in a noticeable amount (about 1.5 wt %) appears only natural and should be attributed to the specific conditions of its preparation.

It is known [7, 15] that detonation of charges of mixed explosives with a negative oxygen balance in a nonoxidizing medium gives rise to formation of detonation soot representing a mixture of nanodiamond and non-diamond forms of carbon contaminated by metal-containing impurities in amounts from 0.5 to 8.0%. By properly applying various methods involving chemical isolation of DND from DC, one can remove the non-diamond form of carbon and the metal-containing impurities by 95%, but pure DND still cannot be obtained in this way. The most widely employed method of chemical purification consisting in boiling DC in a solution of CrO_3 in concentrated H_2SO_4 yields DND with a content of metal-containing impurities of about 1.5 wt %. This entails introduction of the chromium impurity into the samples; as for the iron, which is a major technological contaminant of DND, it remains detectable in concentrations less than 0.5 wt %.

It should be stressed that LND samples revealed the largest carbon content (more than 97 wt,% for sample 1) and turned out to be least contaminated by metal impurities, although after synthesis they were not subjected to any chemical purification.

Figure 1 demonstrates the diffraction pattern for sample 3.

The diffraction graphs are similar for all LND samples: indeed, they all feature broadened diffraction maxima at the angles $2\theta = 53.9°$, 75.3°, 91.5°, and 119.5°, respectively, and a narrow weak maximum deriving from an impurity at the angles $2\theta \approx 27°$. The data obtained for the elemental composition permit a suggestion that the samples contain quartz as an impurity in insignificant amounts. It most likely contaminated the sample during transportation.

Interestingly, a similar diffraction pattern was observed by us repeatedly in samples of detonation diamonds [16]. An analysis of the position and half-width of the diffraction maxima, as well as comparison of diffraction curves of LND and DND samples leads one to the conclusion that the samples under study are actually a polycrystalline diamond material with a lattice parameter $a = 0.3575 \pm 0.0001$ nm. Note that all the LND samples studied have the same lattice parameter (see table), slightly larger than that characteristic of standard diamond materials ($a = 0.35667$ nm).

A comprehensive analysis of the shape of the diffraction curves and of the variation with angle of the broadening of the maxima permits a conclusion bearing on the characteristic size of the coherent scattering region (CSR) in the sample and, indirectly, on the particle size distribution. Indeed, if a diffraction maximum has a shape fitted satisfactorily by one of the well known functions (Lorentz or Cauchy, for instance), the particles have a normal distribution in size with an average size equal to that of the CSR.

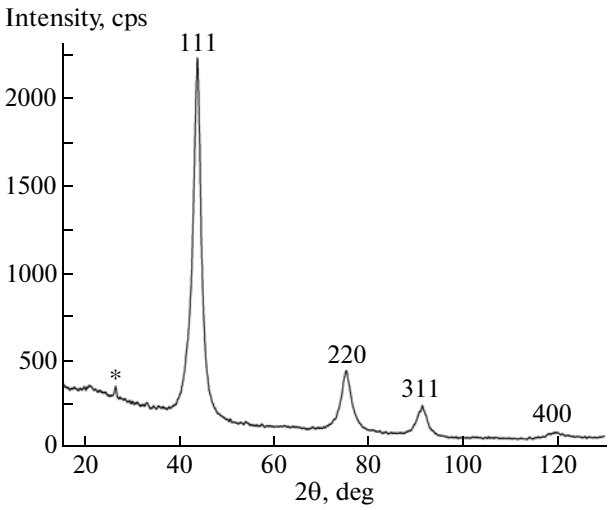

Fig. 1. Diffraction pattern for sample 3. Miller indices identify the maxima corresponding to dispersion from a cubic body-centered lattice with the parameter $a = 0.3575$ nm for diamond $(111)_D$, $(220)_D$, $(311)_D$, $(400)_D$ and a maximum $(10.1)_Q$ corresponding to a quartz impurity. CuK_α radiation ($\lambda = 1.541$ Å).

The diffraction maxima of all LND samples differ in shape from the Cauchy curve, and the CSR measures 5.7, 5.3, and 5.0 nm, respectively (see table). This permits a conclusion that LND samples feature a characteristic particle distribution in size different from the normal one, the CSR of sample 3 being the smallest.

The conclusion that the samples represent powders of nanosized diamond particles with a polydisperse size distribution is borne out by transmission electron microscopy data. Figures 2a and 2b display bright-

Parameters of the particle structure and porous structure of ND agglomerates obtained by PLA and detonation synthesis

Characteristics	1[a]	2[a]	3[a]	4[b]
Lattice parameter a, nm	0.3575	0.3575	0.3575	0.3563
CSR, nm	5.7	5.3	5.0	4.7
S_s, m^2/g	230	255	279	274
	216[c]	221[c]	245[c]	250[c]
V_Σ for $P/P_0 \longrightarrow 1$, cm^3/g	0.78	0.86	0.87	1.14
d_p, g/cm^3	2.95	2.94	2.89	2.94
D, nm	8.8	8.0	7.4	7.4

[a] LND samples.
[b] DND sample.
[c] Data obtained from the Ar adsorption isotherm at 87 K.

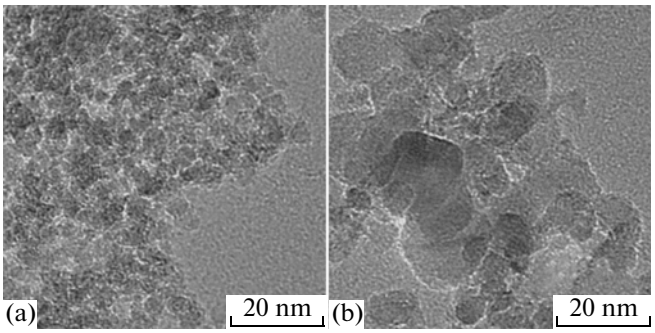

Fig. 2. Electron microscope images of sample 1: (a) part of LND sample with the most characteristic ND particle size range of 4–7 nm and (b) part of the sample with large LND particles (up to 20 nm).

field images of various parts of sample 1. We clearly see that particles recorded in different regions differ strongly in size: indeed, in Fig. 2a there are many small particles, smaller than 5 nm, whereas in Fig. 2b the field contains several large particles with sizes ranging up to 20 nm. A series of similar microphotographs were used to draw histograms of cluster distributions in size for all LND samples, which are demonstrated in Fig. 3.

As seen from the histograms, all the samples have a polydisperse particle distribution in size, the larger part of the material being made up of 3–4-nm particles.

Note that in contrast to the DND sample featuring a more narrow particle distribution in size (Fig. 3), in the LND samples the fraction of particles of a larger size is fairly large. This is particularly evident in the histogram of sample 2, which reveals three maxima for 3, 7, and 13 nm. The histogram of sample 1 demonstrates that particles with sizes from 9 nm to 16 nm can be met in it fairly frequently and, significantly, that one can observe in it even particles larger than 20 nm (not shown in the histogram).

A comparison of the CSR parameters and histograms of particle distributions in size (Fig. 3) suggests that the variation of the composition of targets and of their treatment regimes in NDs prepared by the PLA method brings about noticeable changes in the size distribution of nanoparticles.

The direct image of the structure of sample 1 obtained by TEM reveals that both small and large particles of the LND sample are actually perfect nanodiamond crystallites (see Fig. 4). One clearly sees in the image the {111} crystallographic planes of diamond. Note that the nanodiamond particles measure 5 nm and 10 nm.

In Fig. 5, IR absorption spectra of LND samples (1–3) are compared with those of the sample obtained by detonation synthesis (4). The structure of the spectra repeats itself, the only exclusion being a narrow peak at 1384 cm^{-1} seen in the LND spectra. In the spectrum of sample 3 its intensity is 1.5–2 times higher than in those of samples 1 and 2.

The universally adopted data [4, 17, 18] on the vibrational absorption spectra of NDs demonstrate convincingly the presence of the following functional groups:

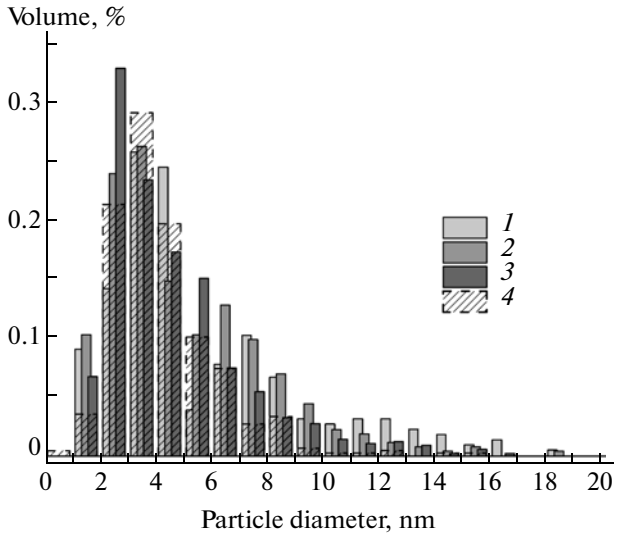

Fig. 3. Histogram of ND particle size distribution. The height of solid bars reflects the fraction of particles of the corresponding diameter for (*1–3*) LND samples and the height of slashed bars, for (*4*) DND sample. The histograms are numbered in accordance with the numbers of samples in the table.

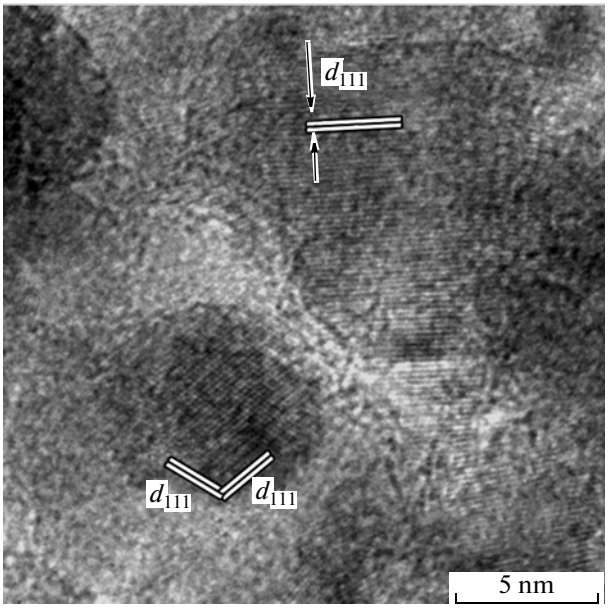

Fig. 4. High-resolution electron microscope image of the structure of sample 1. One clearly sees {111} planes of diamond structure ($d_{111} = 0.205$ nm).

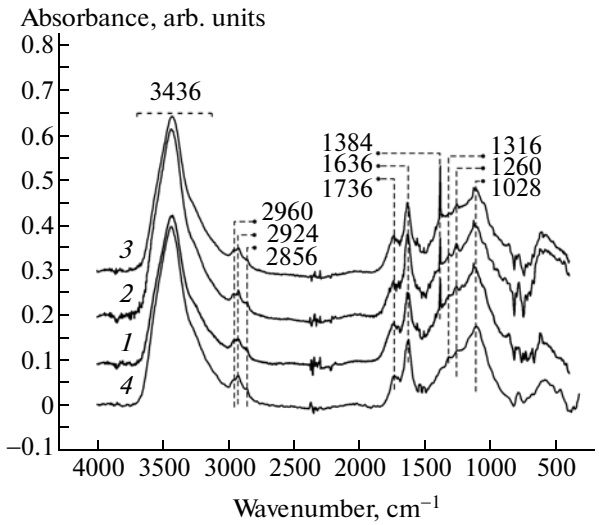

Fig. 5. IR absorption spectra of ND samples. The curves are numbered in accordance with the numbers of samples in the table: (*1*–*3*) LND samples and (*4*) DND sample.

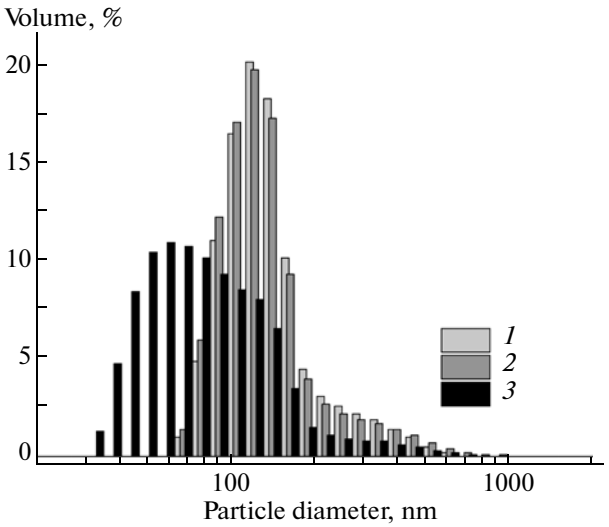

Fig. 6. Histogram of size distribution of ND agglomerates in water solutions of LND samples. Numbers on the histogram are those of samples in the table: column heights identify the fraction of ND agglomerates of particles of the corresponding diameter for sample *1*—light gray histogram, that for sample *2*—gray, and for sample *3*—dark gray.

(i) a broad band peaking at 3436 cm^{-1}: stretching vibration of the O–H bond, primarily of water sorbed by the KBr disk and the sample proper;

(ii) 2960, 2924, 2856 cm^{-1}: stretching vibrations of methyl and methylene groups ($C-H_3$, $C-H_2$);

(iii) 1736 cm^{-1}: stretching vibrations of the C=O double bond of the carboxyl group;

(iv) 1636 cm^{-1}: bending vibrations of sorbed water.

Individual vibrations in the 1600–800 cm^{-1} region are only poorly resolvable. One can single out the 1316–1260 cm^{-1} subband dominated by bending vibrations of hydrogen-containing groups, and the absorption band with the maximum at 1128 cm^{-1} is ordinarily assigned to C–O bond vibrations (irrespective of the functional group to which this bond belongs).

A comparison of the spectra (Fig. 5) shows that all the ND samples studied, both of the laser and the detonation synthesis have surface groups of similar composition. The main difference consists in that the spectrum of the detonation ND sample does not contain the 1384 cm^{-1} peak (spectrum 4). There is, however, evidence [4] of the presence of similar absorption in DND prepared by dry synthesis and subjected to oxidizing purification in hot nitric acid, as well as in commercial DND produced by Altai (Biysk). The presence of this peak was considered as originating from absorption of alcohol-containing C–O–H groups bound to nanodiamond surface, which are intermediates of the oxidizing reaction.

We also observed this peak in a study of DND which underwent chemical modification by ions of divalent copper [17]. The starting material in the latter case was industrial DND subjected to additional acidic purification. The peak was observed in both acid-purified and in chemically modified DND. The data presented in this paper were obtained from DND prepared by boiling DC in the solution of CrO_3 in sulfuric acid, and this is what accounts for the absence of the peak at 1384 cm^{-1}.

Note that there is a scatter of up to 10 cm^{-1} in the position of this peak attributed to C–O–H bending vibrations in different compounds [19].

In an analysis of the 1384 cm^{-1} peak we have to bear in mind the narrow profile of the maximum and that it always occupies the same position in different LND samples. This suggests that the peak at 1384 cm^{-1} in LND absorption spectra relates only to vibrations in specific groups which contain C–O–H, a feature most typical of primary alcohols and carboxylic acids having the $-CH_2-$ link in the alpha position.

Considering the technique employed in LND synthesis, the presence in the spectra of samples 1–3 of the peak at 1384 cm^{-1} may suggest the presence of acetogroups which became attached to ND surface in the course of chemical reactions in one of the synthesis stages [20]. To obtain a substantiated answer, one would have, however, to perform additional studies.

Figure 6 displays histograms of the distribution of ND agglomerates in size obtained by DLS in a water solution of LND samples. We readily see that samples 1 and 2 form agglomerates more than 60 nm in size for an average size of 150 nm. Agglomerates in sample 3 are smaller; indeed, the sizes vary here from 30 nm to 500 nm, with an average of about 60 nm. This behavior

is typical of DND also, provided they are not subjected to a special procedure of deaggregation.

The mechanisms involved in DND aggregation are described in considerable detail [21], and one of the factors here is the surface coverage of functional groups characteristic of DND. DND agglomerates are known to possess an intricate hierarchical structure; indeed, they are made up of aggregates 30–50 nm in size difficult to disrupt, which combine to form more loose aggregates of a large size. It is possible to produce stable suspensions of DND with agglomerates about 30 nm in size by proper methods of fractionation of water DND suspensions.

In comparing experimental data obtained for LND with available results on the size of particles in DND, it should be stressed that for sample 3 the water solution of agglomerates in LND measuring about 60 nm was prepared without employing special methods of fractionation. It is possible that the specific structure of agglomerates in sample 3 (compared with samples 1 and 2) formed as a result of reducing to one half the separation between hydroshocks on the target surface.

Drying ND suspensions produces powders with a characteristic porous structure made up of primary nanodisperse particles combined in agglomerates. The pores in such systems are essentially spaces separating the primary particles. In this case, the specific surface area S_s is determined by the size of the primary particles and extent of the aggregation joining them. The shape of the pores depends on the shape and size of the primary particles, and their specific volume V_Σ, on the size of the particles and their packing density.

In determination of the specific surface area, two adsorptives were used, nitrogen at 77 K and argon at 87 K, which permitted us to form a judgment of the relative size of micropores in ND agglomerates.

Assuming the agglomerate to be composed of spherical particles of the same size, the particle size can be derived from the values of two characteristics: specific surface area S_s and the pycnometric density d_p from the expression for the volume-surface mean diameter of the particles [22]: $D = 6 \times 10^3/d_p S_s$, where d_p is the pycnometric density for helium, and S_s is the specific surface area. The values of the above quantities needed for calculation and the results obtained are listed in the table.

As seen from the table, the values of S_s obtained for the two adsorptives are close in magnitude, but slightly smaller for argon than for nitrogen. There is nothing strange in the latter estimate and it correlates with the different ionic radii of these elements. It is essential that in absolute magnitude of specific surface areas samples 3 (LND) and 4 (DND) do not differ within the accuracy of the method used.

The smaller pycnometric density in the LND studied compared with the tabulated data for the diamond of static synthesis ($d_p \approx 3.3$ g/cm^3) provides one more evidence for the presence of pores in LND powders as a result of their aggregation.

The values of the specific surface area S_s and pore volume V_Σ obtained [23] for the DC containing 0.39–0.74 fraction of diamond carbon prepared by detonation synthesis of various explosives were found to be 245–375 m^2/g and 0.78–1.15 cm^3/g, respectively, which correlates with our data for LND.

The volume-surface size D of a particle in the agglomerate exceeds the CSR dimensions derived from X-ray diffraction data for each of the samples. This result correlates well with the data [24] suggesting the presence of absorbed water on DND surface in water solutions. Incidentally, the size of a particle, allowing for the layer of "nanowater" coating its surface, was 7.2 to 8.6 nm.

It should be stressed here that all the powder samples studied were obtained by drying from their water solutions. It thus follows that LND samples demonstrate both the propensity to absorbing water from the surrounding atmosphere and the presence of closed pores, in which water persists even after a sample has been dried to constant mass at 105°C. This provides one more evidence for both the surface coverage of particles and the structure of agglomerates in LND and DND samples made up of such particles under drying being similar.

5. CONCLUSIONS

We have reported on a study of ND obtained by a radically novel method of laser treatment of a specially prepared carbon target. It has been shown that ND particles have an average size of about 5 nm and may be considered as a material similar in many parameters to detonation nanodiamond: indeed, they represent diamond nanoparticles with a surface coating consisting primarily of oxygen-containing groups. It is known that this coverage defined the main physicochemical properties of DND [3, 21, 25, 26]. Also, LND samples demonstrate a higher purity compared with a standard DND sample produced presently on a commercial scale. It has been shown that the proposed technology makes possible proper monitoring of particle size and of the composition of functional groups on the surface of LND particles.

Among the essential factors that are capable of influencing the LND structure are the composition of the specially prepared target; optical and mechanical characteristics of the liquid into which the target is placed; the duration, shape, and energy of the pulse; and the distance from the pulse focus to the target being treated.

Efforts are planned to be directed at a proper selection of these technological parameters, which will make possible preparation of LND samples with the characteristics required for a specific application.

ACKNOWLEDGMENTS

We are grateful to A.V. Shvidchenko for the presented data.

The study was performed with the equipment provided by the Regional Joint Use Center "Materials Science and Diagnostics in Advanced Technologies" and was supported by the Russian Foundation for Basic Research (project no. mol_a 12-03-31231) and the Ministry of Education and Science of the Russian Federation.

REFERENCES

1. *Ultrananocrystalline Diamond: Synthesis, Properties and Applications*, Ed. by O. A. Shenderova and D. M. Gruen (William Andrew, Norwich, New York, 2006).
2. *Nanodiamonds: Applications in Biology and Nanoscale Medicine*, Ed. by D. Ho (Springer-Verlag, New York, 2009).
3. M. Baidakova and A. Vul, J. Phys. D: Appl. Phys. **40**, 6300 (2007).
4. A. Krüger, F. Kataoka, M. Ozawa, T. Fujino, Y. Suzuki, A. E. Aleksenskii, A. Y. Vul, and E. Ösawa, Carbon **43**, 1722 (2005).
5. O. A. Williams, J. Hees, C. Dieker, W. Jager, L. Kirste, and C. E. Nebel, ACS Nano **4**, 4824 (2010).
6. A. E. Aleksenskiy, E. D. Eydelman, and A. Y. Vul', Nanosci. Nanotechnol. Lett. **3**, 68 (2011).
7. V. Yu. Dolmatov, Usp. Khim. **70**, 687 (2001).
8. J.-P. Boudou, P. A. Curmi, F. Jelezko, J. Wrachtrup, P. Aubert, M. Sennour, G. Balasubramanian, R. Reuter, A. Thorel, and E. Gaffet, Nanotechnology **20**, 235602 (2009).
9. C. X. Wang, P. Liu, H. Cui, and G. W. Yang, Appl. Phys. Lett. **87**, 201913 (2005).
10. S. R. J. Pearce, S. J. Henley, F. Claeyssens, P. W. May, K. R. Hallam, J. A. Smith, and K. N. Rosser, Diamond Relat. Mater. **13**, 661 (2004).
11. G. Askar'yan, A. Prokhorov, G. Chanturiya, and G. Shipulo, Sov. Phys. JETP **17**, 1463 (1963).
12. A. M. Panich, A. I. Shames, B. Zousman, and O. Levinson, Diamond Relat. Mater. **23**, 150 (2012).
13. N. R. Wilson, P. A. Pandey, R. Beanland, R. J. Young, I. A. Kinloch, L. Gong, Z. Liu, K. Suenaga, J. P. Rourke, and S. J. York, ACS Nano **3**, 2547 (2009).
14. S. Brunauer, P. H. Emmett, and E. Teller, J. Am. Chem. Soc. **60**, 309 (1938).
15. V. Dolmatov, *Ultradispersed Diamonds of Detonation Synthesis* (St. Petersburg State Polytechnical University, St. Petersburg, 2003) [in Russian].
16. A. Y. Vul, in *Ultrananocrystalline Diamond: Synthesis, Properties and Applications*, Ed. by O. A. Shenderova and D. M. Gruen (William Andrew, Norwich, New York, 2006), p. 379.
17. V. Y. Osipov, A. E. Aleksenskiy, A. I. Shames, A. M. Panich, M. S. Shestakov, and A. Y. Vul, Diamond Relat. Mater. **20**, 1234 (2011).
18. I. Larionova, V. Kuznetsov, A. Frolov, O. Shenderova, S. Moseenkov, and I. Mazov, Diamond Relat. Mater. **15**, 1804 (2006).
19. SDBSWeb:http://riodb01.ibase.aist.go.jp/sdbs/ (National Institute of Advanced Industrial Science and Technology, Tokyo).
20. G. Yang, Prog. Mater. Sci. **52**, 648 (2007).
21. A. E. Aleksenskiy, M. V. Baidakova, V. Y. Osipov, and A. Y. Vul', in *Nanodiamonds: Applications in Biology and Nanoscale Medicine*, Ed. by D. Ho (Springer-Verlag, New York, 2009), p. 55.
22. S. Gregg and K. Sink, *Adsorption, Surface Area and Porosity* (Academic, New York, 1982; Mir, Moscow, 1984).
23. K. S. Baraboshkin, N. V. Kozyrev, and V. F. Komarov, Polzunovskii Vestn., No. 2, 13 (2006).
24. M. V. Korobov, N. V. Avramenko, A. G. Bogachev, N. N. Rozhkova, and E. Ösawa, J. Phys. Chem. C **111**, 7330 (2007).
25. A. Krueger and D. Lang, Adv. Funct. Mater. **22**, 890 (2012).
26. V. N. Mochalin, O. Shenderova, D. Ho, and Y. Gogotsi, Nat. Nanotechnol. **7**, 11 (2011).

Translated by G. Skrebtsov